ISSN: 1813-4890

Numerical Analysis of the Screening Efficiency of a Tapered Cylindrical Vibrating Screen

Yujia Li [1], Weisong Yu [1], Tao Ren [2], Weiye Zhuang [1], Zheyi Jin [1]

[1] School of Mechatronic Engineering, Southwest Petroleum University, and the Oil and Gas Equipment Technology Science and Technology Information Resource Sharing Service Platform of Sichuan Province, Chengdu 610500, China

[2]State Key Laboratory of Geohazard Prevention and Geoenvironment Protection, and School of Mechanical and Electrical Engineering, Chengdu University of Technology, Chengdu 610059, China

Abstract

The tapered cylindrical vibrating screen offers distinct advantages across industries such as mining, chemical processing, and construction materials, owing to its unique geometric design and dynamic screening mechanism. This study elucidates the impact of key parameters like amplitude, rotational speed, and frequency on screening efficiency and particle movement by using numerical simulations with the Discrete Element Method. The results demonstrate that amplitude significantly impacts screening efficiency, with an optimal range that maximizes performance. Increasing rotational speed enhances particle dispersion and screening efficiency; however, excessive speeds reduce particle retention time on the screen, decreasing thoroughness. Furthermore, changes in frequency affect particle velocity and jumping intensity, with proper frequency settings improving efficiency and reducing screen clogging. This analysis offers valuable theoretical insights and technical guidance for the practical application and design of cylindrical vibrating screens with taper by investigating their screening mechanisms and operational parameters.

Keywords

Conical Cylindrical Vibrating Screen, EDEM, Discrete Element Method, Particle Simulation, Numerical Analysis.

1. Introduction

In modern industrial production and material handling, vibrating screening technology plays a pivotal role, with its performance directly influencing production efficiency and product quality. As a key method for material classification, sorting, and purification, vibrating screening relies on mechanical vibrations that induce materials to jump, tumble, and slide across the screen surface, facilitating particle separation by size [1-3]. With advancements in science and technology, various vibrating screening devices have been developed. The authors proposed a tapered cylindrical vibrating screen which couples rotation and vibration motion, incorporates a conical design into the traditional cylindrical screen, allowing particles to move upward during screening [4-5]. This innovation enhances material separation, reduces clogging, and improves screening efficiency, making it highly promising for practical applications. Thus, the performance optimization of the tapered cylindrical vibrating screen is of great practical significance. Optimizing the performance of such a vibrating screen demands a comprehensive consideration of various factors. By means of numerical simulation, a profound examination of the impact of assorted parameters on screening performance can be conducted. Thereby, providing a theoretical basis and technical support for the design optimization and engineering application of vibrating screens [6-8].

ISSN: 1813-4890

DEM technology permits the simulation of particle motion trajectories along with force interactions on the screen surface, thereby facilitating the prediction of screening efficiency within the context of different parameter combinations [9-12]. In recent years, scholars have carried out extensive and profound research regarding vibrating screening technology and have attained a series of significant outcomes. Jahan et al. [13] employed the DEM solver of lights to conduct further simulations of the double-deck banana screen on both industrial and laboratory scales. They probed into the influence of design and operating parameters on screening performance. Zhao et al. [14] carried out analogous DEM simulations concerning circular vibrating screens. They dissected the independent impact of diverse vibration parameters on screening efficiency. Jafari and Nezhad [15] utilized DEM to simulate linear vibrating screens and disclosed the influence of distinct parameters on screening efficiency and screen hole wear. Currently, research on the performance optimization of tapered cylindrical vibrating screens under rotating and vibrating coupling conditions is relatively scarce, especially studies on the influence of multiple variables (such as amplitude, rotational speed, and frequency) on the screening process, which are still in the exploratory stage.

Currently, the research on the performance optimization of the tapered cylindrical vibrating screen under the coupled rotational and vibrational conditions is rather scarce. Specifically, the exploration of the impacts of multiple variables, including amplitude, rotational speed, and frequency, on the screening process is insufficient. Accordingly, this research is committed to conducting a systematic analysis of the dynamic behavior exhibited by the tapered cylindrical vibrating screen within the context of coupled rotational and vibrational states, employing the Discrete Element Method as the analytical tool. Through an in-depth investigation of the influence of crucial parameters on screening efficiency and material movement trajectories, this research offers scientific insights and technical support for enhancing the performance of vibrating screens.

2. Theoretical Model and Parameter Settings

2.1. Simulation Model

When conducting a simulation study on the dynamic behavior of a vibrating screen, the selection of the contact model is of crucial importance. In the research, the Hertz–Mindlin model (No-Slip) is adopted. This model occupies an extremely central position in the exploration of granular material mechanics, with its core concentrating on the contact mechanical phenomena among particles.

In the context of the normal contact force, in accordance with the Hertz theory, it provides a fundamental understanding of the contact mechanics between elastic bodies[16].

The Hertz theory is a well established approach for analyzing the contact between two curved surfaces. It assumes that the contacting bodies are elastic and that the contact area is small compared to the size of the bodies[17].

Mathematically, the normal contact force F_n between two spherical bodies of radii R_1 and R_2, with a modulus of elasticity E and Poisson's ratio ν, and a compressive displacement δ is given by the Hertzian contact formula[18,19]:

:

$$F_n = \frac{4}{3}E^*\sqrt{R^*}\delta^{3/2} \tag{1}$$

$$\frac{1}{E^*} = \frac{1-v_1^2}{E_1} + \frac{1-v_2^2}{E_2} \tag{2}$$

$$\frac{1}{R^*} = \frac{1}{R_1} + \frac{1}{R_2} \tag{3}$$

In which E* denotes the equivalent elastic modulus, while R*stands for the equivalent radius. Here,δ signifies the normal compression, that is, the normal displacement.

The tangential contact force formula, under no-slip conditions, follows Coulomb's friction law and Mindlin's theory. The tangential force F_t can be expressed as:

ISSN: 1813-4890

$$F_t = -k_t \Delta S \quad (4)$$

$$k_t = 8G * \sqrt{R * \delta} \quad (5)$$

$$\frac{1}{G^*} = \frac{2-v_1}{G_1} + \frac{2-v_2}{G_2} \quad (6)$$

This formula distinctly manifests the interrelation between the normal contact force and the elastic traits (elastic modulus and Poisson's ratio) of the granular substance, along with the contact deformation. It implies that the normal contact force escalates in tandem with the augmentation of the contact deformation magnitude and is intricately associated with the elastic attributes of the particles. With respect to the tangential contact force, Mindlin expanded upon it grounded on the Hertz theory. When two particles are in contact and exposed to a tangential force, the magnitude of the tangential force is contingent upon multiple elements, including the normal contact force, the inter-particle frictional coefficient, and the relative displacement of the particles. Denote the tangential contact force as F_t and the coefficient of friction as μ. In the scenario where no relative slippage transpires, the tangential contact force and the tangential displacement present a particular elastic correlation, analogous to the connection between the elastic force and displacement of a spring. Once the tangential force exceeds the limiting friction force (the limiting friction force is equal to the product of the friction coefficient and the normal contact force, that is $F_t \leq \mu F_n$), relative sliding will occur between the particles[20].

By using the Hertz–Mindlin (No-Slip) model, the force situation and motion trajectory of particles during the working process of a tapered cylindrical vibrating can be simulated more accurately, thereby enabling an in-depth analysis of its screening efficiency and material distribution [21]. The design characteristics of the tapered cylindrical vibrating make this model particularly suitable for analyzing the contact behavior in such vibrating screens, as this model can handle well the complex mechanical environment under the coupling condition of rotation and vibration of the vibrating screen [22, 23].

2.2. Definition of Screening Efficiency

Screening efficiency is a key metric in the screening operation. It shows what fraction of the total input particles can make it through the screen of a vibrating screen. Essentially, you figure it out by taking the number of particles that do pass through the screen, dividing that by the total number of particles you started with, and then multiplying by 100% to get a percentage. To work it out, you first need to know the total amount of particles going into the vibrating screen. Then, after the screen has been running for a bit, you count the number of particles that came out on the other side. Plug those numbers into the formula and you've got the screening efficiency. A high value means the screen is doing a good job of separating the particles according to size, while a low value might mean the holes in the screen are the wrong size or that you need to tweak other settings like vibration intensity or running time. Keeping an eye on this efficiency in real-world applications lets you pick the best screen and adjust how it's run to make better quality products faster.

$$P_L = \frac{NL}{N_T} \times 100\% \quad (7)$$

In this context, N_L represents the quantity of particles that traverse the screen, while N_T denotes the overall count of valid particles that have been generated.

2.3. Parameter Settings

The prototype of the tapered cylindrical vibrating screen has a length of 2m, a cylinder diameter of 260mm, a cone angle of 1°, and a mesh size of 150 mesh as shown in Figure 1. However, due to the limitations of computer performance, it is not feasible to process excessively large data. Therefore, the authors have simplified the entire system to a conical screen mesh plus particles and reduced the size of the vibrating screen to a cone with a cone angle of 1°, small hole diameter of 1mm, length of 200mm, and cylinder diameter of 26mm, as shown in
Figure 2.

ISSN: 1813-4890

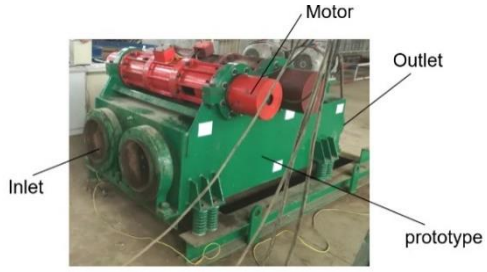

Fig 1 Tapered cylindrical vibrating screen prototype

Considering the existing computer performance, in order to improve the calculation rate, all simulated particles adopt single spherical particles with diameters of 1.2mm, 1mm, 0.8mm, 0.6mm, and 0.4mm, distributed in a fixed ratio of 20% each. The material properties of particles and the screen mesh are shown in Table 1. The mechanical properties between particles and particles, as well as particles and materials, are shown in Table 2.

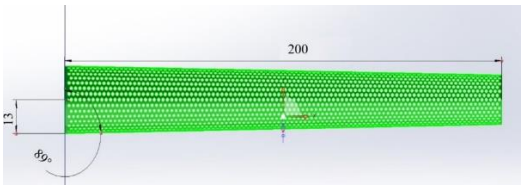

Fig 2 Model parameters

Table 1 Material Properties

Material Property	Poisson's Ratio	Density	Shear Modulus
Particle	0.2	2600kg/m3	50MPa
Screen Mesh	0.3	7800kg/m3	70GPa

Table 2 Interaction Forces Between Materials

Material	Coefficient of Restitution	Static Friction Coefficient	Rolling Friction Coefficient
Particle-Particle	0.0003	0.44	0.01
Particle-Screen Mesh	0.03	0.5	0.002

This simulation aims to explore the influence of rotational speed, amplitude, and frequency on particle screening effectiveness. Therefore, these three variables are treated as single controlled variables. Four sets of simulations are conducted for each variable, as shown in Table 3.

Table 3 Simulation Parameters

Frequency (Hz)	Amplitude (mm)	Rotational Speed (rpm)
15, 20, 25, 30	2, 3, 4, 5	0, 10, 20, 30

3. Simulation Results and Analysis

(1) Impact of Amplitude on Vibrating Screen Performance

Figures 3and 4 show the screening efficiency and the average particle velocity along the axial direction of the screen under constant rotational speed of 30 rpm and a frequency of 20 Hz, with varying amplitudes (2mm, 3mm, 4mm, and 5mm). As the amplitude increases, the vibration of the screen surface becomes more intense, resulting in greater vibrational forces acting on the particles, which accelerates their movement across the screen. A larger amplitude increases particle displacement on the screen surface and raises the collision frequency between particles and screen apertures, promoting both particle separation and forward movement.

As shown in Figure 4, it can be seen that the amplitude directly affects screening efficiency. Smaller amplitudes result in weaker particle throwing intensity, causing particle clusters to remain more compact, reducing the chances of particles making contact with the screen surface, and thereby lowering the screening efficiency.

ISSN: 1813-4890

When the amplitude is 2mm, the screening efficiency reaches its highest value of 22.49%. However, due to the tapered shape of the screen, particles tend to climb upward with the vibration, increasing the time it takes for them to reach the outlet. As shown in Figure 5(a), the small amplitude results in a low axial velocity for the particles, preventing them from successfully climbing the slope, causing many particles to rebound and accumulate in the middle of the screen, with a small portion flowing back out of the inlet.

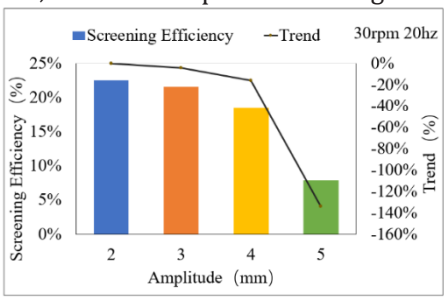

Fig 3 Sieve rates of different amplitudes

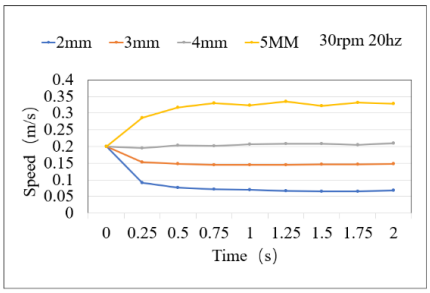

Fig 4 The average velocity of the particles along the axial direction of the sieve barrel

As the amplitude increases, the throwing intensity and velocity of the particles increase, allowing particles to spread out more easily. This leads to an enhanced interaction between the fine particles and the screen surface, consequently promoting the screening efficiency. However, in the case where the amplitude reaches an excessive level, a reduction in the screening efficiency is observed. At an amplitude of 5mm, particles experience intense jumping on the screen surface, with their jump height exceeding the vibration cycle of the screen, which reduces the contact time between the particles and the screen, significantly lowering the screening efficiency. Therefore, there is an optimal amplitude range that maximizes screening efficiency.

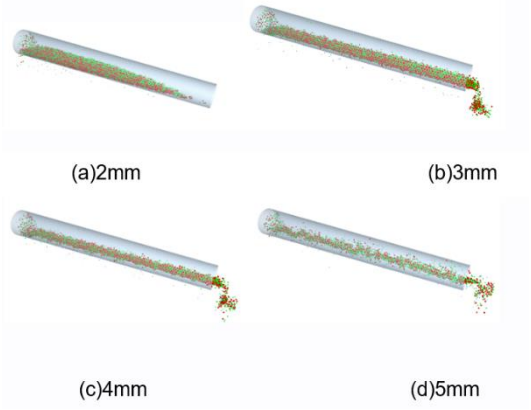

Fig 5 Screening for different amplitude

(2) Impact of Rotational Speed on Vibrating Screen Performance

Figures 6 and 7 show the screening efficiency and the average particle velocity along the axial direction of the screen under constant amplitude of 3mm and frequency of 20 Hz, with varying rotational speeds (0 rpm, 10 rpm, 30 rpm, and 50 rpm). The rotational speed of the cylindrical vibrating screen does not significantly affect the particle velocity, with increased rotational speeds slightly reducing the average particle velocity along the axial direction of the screen.

ISSN: 1813-4890

When the screen's rotational speed is 0, meaning only elliptical vibration occurs, the particles move the fastest along the axial direction, reaching up to 0.155 m/s, and some particles reach the outlet within 0.66 seconds. However, this does not allow for sufficient particle screening, resulting in a screening efficiency of only 19.53%.

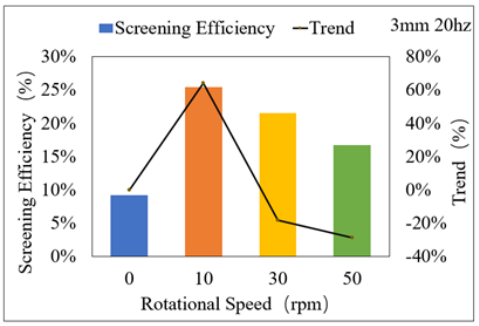

Fig 6 Sieving rate at different speeds

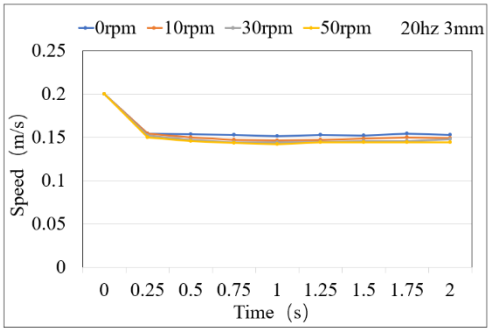

Fig 7 The average velocity of the particles along the axial direction of the sieve barrel

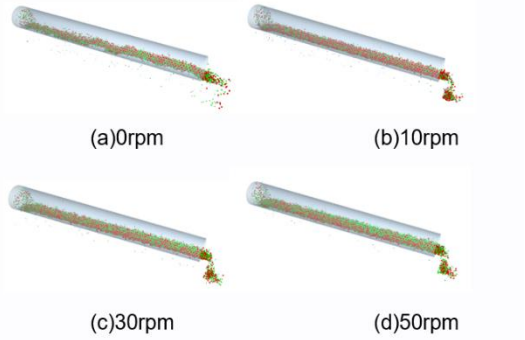

Fig 8 Screening for different speeds

As the rotational speed increases, the centrifugal force acting on the particles also increases, accelerating their tangential velocity along the cylindrical screen and increasing the material flow during the screening process. As shown in Figure 8, the higher rotational speed alters the particle motion trajectory, making it more complex and vigorous. This helps to break particle adhesion and agglomeration, improving screening efficiency. The highest screening efficiency, 25.49%, occurs at a rotational speed of 10 rpm. However, further increasing the rotational speed reduces the residence time of particles on the screen surface, compromising the adequacy of the screening process and lowering the screening efficiency.

(3) Impact of Frequency on Vibrating Screen Performance

Figures 9 and 10 illustrate the situations of the screening efficiency and the average axial velocity of particles along the screening cylinder, respectively, under constant rotational speed of 30 rpm and amplitude of 3 mm, but with varying frequencies of 15 Hz, 20 Hz, 25 Hz, and 30 Hz. When the frequency is set to 15 Hz, the through-screen rate reaches 23.04%, however, the average axial velocity of particles along the screening cylinder nearly drops to zero. The vibration of the screening surface becomes sluggish, leading to a reduction in the movement speed and jumping intensity of particles on the screen. Consequently, the dispersion and

ISSN: 1813-4890

collision among particles decrease, minimizing the opportunities for particles to come into contact with the screening mesh, which in turn lowers the screening efficiency. Moreover, low-frequency vibration is more prone to causing mesh clogging, further diminishing the screening efficiency, as depicted in Figure 12.

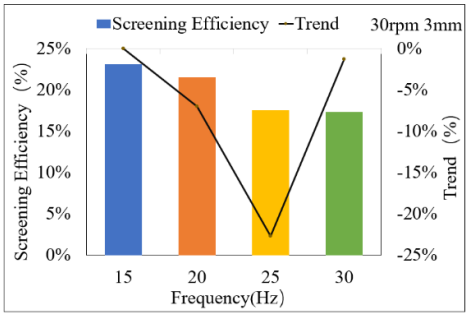

Figure 9 Sieve rates at different frequencies

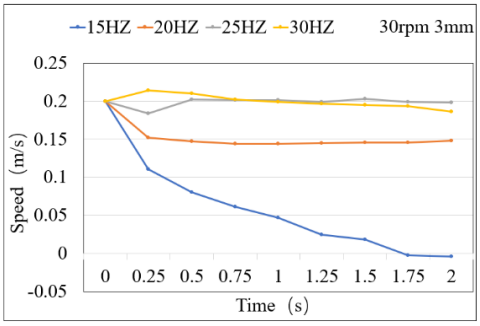

Figure 10 The average velocity of the particles along the axial direction of the sieve barrel

Figure 11 Screening scenarios at different frequencies

As the frequency continues to increase, the average axial velocity of particles along the screening cylinder significantly rises, while the through-screen rate experiences a slight decline. This may be attributed to the excessively high vibration frequency, which results in a shortened residence time of particles on the screening surface. Consequently, some particles may be discharged from the screen without undergoing sufficient screening, thereby affecting the precision and effectiveness of the screening process.

4. Conclusions and Discussions

This study conducted a systematic simulation analysis of the tapered cylindrical vibrating screen under coupled rotational and vibrational conditions using the Discrete Element Method (DEM) in EDEM software. Twelve simulation groups were designed to investigate the effects of three variables—amplitude, rotational speed, and frequency—on the performance of the tapered cylindrical vibrating screen. Each variable was tested at different levels across four simulations to ensure the reliability and accuracy of the results. Main conclusions can be drawn from the work.

(1) The analysis of varying amplitudes reveals that amplitude significantly influences screening efficiency and particle motion. Smaller amplitudes (e.g., 2mm) can ensure a high screening efficiency but may lead to particle accumulation on the screen, reducing overall effectiveness. As the amplitude increases, the throwing intensity of the particles improves, enhancing screening efficiency; however, excessively large amplitudes

(e.g., 5mm) can reduce the contact time between particles and the screen, ultimately decreasing efficiency. Thus, there exists an optimal amplitude range that maximizes screening efficiency.

(2) The study of varying rotational speeds indicated a direct impact of the rotational speed on particle velocity and trajectory. At a rotational speed of zero, particles primarily move along the axial direction of the screen, resulting in low screening efficiency. With an increase in the rotational speed, the centrifugal force acting on the particles accelerates their tangential velocity along the cylindrical screen, promoting particle dispersion and screening. However, excessively high rotational speeds can shorten the residence time of particles on the screen, compromising screening adequacy, with the highest screening efficiency observed at 10 rpm.

(3) The analysis of varying frequencies showed a significant effect on particle movement speed and jumping intensity on the screen surface. While low-frequency vibrations (e.g., 15 Hz) can improve screening efficiency, they also slow down particle movement, leading to potential screen clogging. As frequency increases, particle velocity enhances, but excessively high frequencies (e.g., 30 Hz) can lead to insufficient residence time on the screen, negatively impacting screening accuracy and effectiveness.

The optimal parameter combination for the tapered cylindrical vibrating screen in this study involves an amplitude of 2–3 mm, a rotational speed of around 10 rpm, and a frequency of 15–20 Hz, which collectively maximize screening efficiency while balancing particle movement and retention time. This research contributes significant insights into industrial applications in mining, chemical processing, and construction materials by enhancing the separation performance, reducing clogging, and improving the throughput of vibrating screens through parameter optimization.

Acknowledgments

*Research supported by the National Natural Science Foundation of China (52404063 and 52474004), Sichuan Science and Technology Program (2023YFH0102), and Chengdu Science and Technology Bureau Technology Innovation R&D Project (2022-YF05-00825-SN).

References

[1] Safranyik F, Csizmadia BM, Hegedus A, Keppler I. Optimal oscillation parameters of vibrating screens. J Mech Sci Technol. 2019;33(5):2011-2017.

[2] Yujia Li, Xi Fang, Jinnan Zhang, System and process for mud solid control: U.S Patent 10233707 B2[P]. 2019.03.19,

[3] Yujia Li, Peng Zhao, Li Mo, Tao Ren, and Minghong Zhang. Numerical simulation of particle screening efficiency of large multi-layer vibrating screen based on discrete element method. ARCHIVE Proceedings of the Institution of Mechanical Engineers Part E Journal of Process Mechanical Engineering, 2021.

[4] Wu M, Chen F, Li A, Chen Z, Sun N. A novel vibration isolator for vibrating screen based on magnetorheological damper. J Mech Sci Technol. 2021;35(10):4343-4352.

[5] Elskamp F, Kruggel-Emden H, Hennig M, et al. Benchmarking of process models for continuous screening based on discrete element simulations. Miner Eng 2015; 83: 78–96.

[6] Cleary PW, Sinnott MD and Morrison RD. Separation performance of double deck banana screens – part 1: flow and separation for different accelerations. Miner Eng 2009; 22: 1218–1229.

[7] Cleary PW, Sinnott MD and Morrison RD. Separation performance of double deck banana screens – part 2: quantitative predictions. Miner Eng 2009; 22: 1230–1244.

[8] Makinde OA, Ramatsetse BI and Mpofu K. Review of vibrating screen development trends: linking the past and the future in mining machinery industries. Int J Miner Process 2015; 145: 17–22.

[9] Asbjornsson G, Bengtsson M, Hulthen E and Evertsson, Model of banana screen for robust performance. Miner Eng 2016; 91:66–73.

[10] Jiang H, Zhao Y, Duan C, et al. Kinematics of variable amplitude screen and analysis of particle behavior during the process of coal screening. Powder Technol 2017; 306: 88–95.

[11] Zhao LL, Zhao YM, Bao C, et al. Optimisation of a circularly vibrating screen based on DEM simulation and Taguchi orthogonal experimental design. Powder Technol 2017; 310: 307–317.

[12] Cundall PA and Strack ODL. Discrete numerical model for granular assemblies. Geotechnique 1979; 29: 47–65.

[13] Mi L, Guozhi M and Qing L. Mathematical modeling and optimization of spiral drum screen in the concrete residue recovery system. ARCHIVE Proceedings of the Institution of Mechanical Engineers. Part C: Journal of Mechanical Engineering Science 2020; 234(13): 0954406 22090794.

[14] Cleary PW. Large scale industrial DEM modelling. Eng Comput 2004; 21: 169–204.

[15] A. Jafari, Vahid Saljooghi Nezhad, et al. Employing DEM to study the impact of different parameters on the screening efficiency and mesh wear

[16] . Powder Technol 2016; 301: 126–143.

[17] Zhongjun Yin, et al. Simulation of particle flow on an elliptical vibrating screen using the discrete element method Powder Technology 2016; 63: 443–454.

[18] Zadravec M, Orešnik B, Hriberšek M, et al. Two-step validation process of particle mixing in a centrifugal mixer with vertical axis. ARCHIVE Proceedings of the Institution of Mechanical Engineers, Part E: Journal of Process Mechanical Engineering 2018; 232(1): 29–37.

[19] Zhong WQ, Yu AB, Liu XJ, et al. DEM/CFD-DEM modelling of nonspherical particulate systems: theoretical developments and applications. Powder Technol 2016; 302: 108–152.

[20] Li ZF, Li KY, Ge XL, et al. Performance optimization of banana vibrating screens based on PSO-SVR under DEM simulations. J Vibroeng 2019; 21(1): 28–39.

[21] Wu XQ, Li ZF, Xia HH, et al. Vibration parameter optimization of a linear vibrating banana screen using DEM 3D simulation. Journal of Engineering & Technological Sciences 2018; 50(3): 346–363.

[22] Chen B, Yan JW, Xu CL, et al. DEM simulation and experimental study on the screening process of elliptical vibration mechanical systems. J Vibroeng 2019; 21(8): 2025–2038.

[23] Tang H, Jiang Y, Wang J, et al. Numerical analysis and performance optimization of a spiral fertilizer distributor in side deep fertilization of a paddy field. Proceedings of the Institution of Mechanical Engineers, Part C: Journal of Mechanical Engineering Science 2020.

[24] Dong H, Liu C, Zhao Y, et al. Influence of vibration mode on the screening process[J]. International Journal of Mining Science and Technology, 2013, 23(1): 95-98.

[25] Liu C, Wang H, Zhao Y, et al. DEM simulation of particle flow on a single deck banana screen[J]. International Journal of Mining Science and Technology, 2013, 23(2): 273-277.

[26] Chen B, Yan J, Yin Z, et al. A new study on dynamic adjustment of vibration direction angle for dual-motor-driven vibrating screen[J]. Proceedings of the Institution of Mechanical Engineers, Part E: Journal of Process Mechanical Engineering, 2021, 235(2): 186-196.

Author information

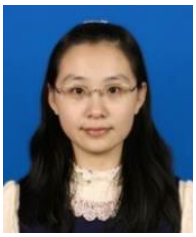

Yu Jia Li is an associate professor and master's supervisor at Southwest Petroleum University (SWPU). She received her B.Sc. in Process Equipment and Control Engineering (2012) and Ph.D. in Mechanical Engineering (2017) from SWPU. From 2015 to 2016, she conducted research on intelligent service robots as a visiting research assistant at the University of Hong Kong. She joined the School of Mechanical and Electrical Engineering, SWPU, in 2017 and completed her postdoctoral research in Petroleum and Natural Gas Engineering in 2020. Her research interests include robotics, mechatronics, petroleum and natural gas equipment, and mechanical system dynamics.

ISSN: 1813-4890

Weisong Yu is a graduate student at the School of Mechanical and Electrical Engineering, Southwest Petroleum University. His current research focuses on the design and optimization of vibrating screens, with an emphasis on performance improvement and dynamic analysis.

Tao Ren is the director of the Intelligent Oil and Gas Equipment Innovation Laboratory at Chengdu University of Technology. He serves as an associate editor for the International Journal of Robotics and Automation (IJRA) and Intelligence & Robotics. He is a candidate for Sichuan Province Academic and Technological Leaders. Specializing in pipeline robot technologies, he has developed over 10 types of robots addressing challenges in buried pipelines, oil and gas collection networks, and municipal underground systems.